Design of On-Orbit Monitoring System for GNSS Signal Quality Based on Intelligent Processing

Qibing Xu(✉), Zhimei Yang, and Lixin Zhang

Xi'an Institute of Space Radio Technology, Xi'an 710100, China

Abstract. Global Navigation Satellite System (GNSS) signal is the medium that provides users with navigation, positioning and timing. The signal quality determines the user's service level and accuracy. GNSS signal quality includes signal continuity and accuracy. Satellite in-orbit service requires timely ground monitoring. There are more and more satellites, and ordinary monitoring methods cannot meet the real-time monitoring. It is necessary to adopt intelligent monitoring methods to realize autonomous on-orbit monitoring. This article introduces a GNSS signal on-orbit intelligent monitoring system, including the composition of the system, intelligent monitoring process, monitorable indicators and monitoring methods. This solution has been applied to current monitoring stations, which greatly simplifies the complexity of monitoring. To improve the efficiency of monitoring.

Keywords: GNSS signal · Quality monitoring · Intelligent processing

1 Introduction

Satellite navigation system is an important space infrastructure, which has brought huge social and economic benefits to mankind. At the same time, it has become an important strategic resource related to national security in the military field. Because of its potential great value, major countries and major groups are competing to develop their own global navigation satellite systems. The Beidou satellite navigation system is an independently developed and independently operated global satellite navigation system that China is implementing. It is compatible with the United States' GPS and Russian satellite navigation systems [1]. GLONASS and the EU's GALILEO system are compatible with the shared global satellite navigation system, and are called the world's four largest satellite navigation systems. In order to provide high-precision navigation and positioning services, navigation satellites must provide continuous, high-precision, and high-integrity signals.

After the satellite is launched, it is necessary to monitor the status of the satellite through the ground monitoring system and carry out the evaluation of the satellite status [2]. The existing ground monitoring system uses monitoring receivers [3]. The monitoring receivers can only monitor the signal continuity, and only provide general and

X. Wang et al. (Eds.): AICON 2021, LNICST 396, pp. 566–578, 2021.
https://doi.org/10.1007/978-3-030-90196-7_49

conventional observation information, and cannot monitor the changes in signal quality indicators. Secondly, due to its hardware resources The monitoring receiver cannot monitor and evaluate all the signals of all visible satellites in the current visible field of view in real time, especially the signal quality cannot be monitored with higher performance. The German Aerospace Research Institute used a 30-m large antenna Monitoring the Galileo satellite system has the disadvantage of not having strong monitoring timeliness, and flexibility also has major difficulties in monitoring flexibility and use [4].

2 GNSS Signal Quality Index System

The measurement of GNSS signal quality is mainly carried out through related methods. At present, navigation signal quality evaluation is widely studied. Scholars have proposed a lot of signal quality evaluation methods, which are more mainstream and widely recognized evaluation indicators, mainly from frequency domain characteristics, time Domain characteristics, correlation domain characteristics, and modulation characteristics are used to evaluate signal quality.

2.1 Frequency Domain Characteristics

The frequency domain characteristic mainly analyzes the power spectrum of the downlink signal, and monitors the change of the transmission power at the same time, which is a basic indicator of signal quality evaluation. The German Aerospace Research Institute used a large 30-m antenna to monitor the Galileo GIOVE-B test satellite in the E1 frequency band with a significant asymmetry of at least 1 dB in the power spectrum [5, 6] (Fig. 1).

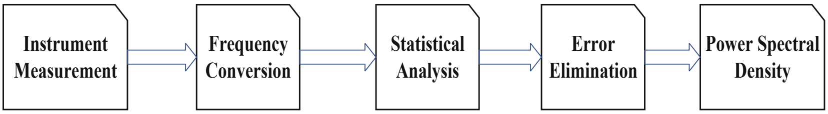

Fig. 1. Signal frequency domain monitoring data analysis process.

Signal power spectrum monitoring mainly uses large-scale monitoring antennas or directly monitors satellite signals during production. Regardless of the monitoring method, the general monitoring process is to collect the radio frequency signal by the instrument, then down-convert the signal, analyze the signal for a period of time, and eliminate the interference and error terms, and finally get the power spectral density of the corresponding signal, the signal. In order to prevent the interference of other signals, when analyzing the power spectral density, a sharp cut filter can be used to analyze only the signal in the main lobe, while increasing the averaging time of the signal to ensure stability.

2.2 Time Domain Characteristics

The signal time domain characteristic mainly analyzes the waveform distortion and constellation diagram of the baseband signal. The baseband signal waveform distortion mainly analyzes the distortion of the baseband signal waveform. First, the collected data is preprocessed, and the baseband waveform "0" and "1" duty ratios are analyzed, and then the time length corresponding to each positive and negative chip of the signal in the code period is counted. And make the difference with the ideal chip length to obtain the time difference series of the "1" and "0" chips and the ideal chip, and finally calculate the standard deviation and mean value of the two time series respectively [2, 5].

At present, there is no effective constellation diagram evaluation method for the more complicated modulation type navigation signals. For example, the eye diagrams commonly used in communication are not suitable for navigation signals. However, the analysis of the constellation diagram can provide an intuitive impression for the evaluation of the signal quality. If the distortion is serious, the corresponding constellation diagram and the constellation diagram of the ideal signal will be obviously inconsistent. It should be noted that when comparing the real signal with the ideal signal, it is necessary to ensure that the effective bandwidth of the two is the same.

2.3 Related Domain Characteristics

After the navigation downlink signal is distorted, the correlation function is distorted, causing pseudorange measurement errors. The correlation function is used to analyze the influence of the transmission channel on the navigation downlink signal ranging performance. First, the software receiver is used to carry out carrier stripping and Doppler removal on the navigation satellite signal to obtain the signal ranging code, and calculate the normalized cross-correlation with the local reference code, which is defined as the following formula:

$$CCF(\tau) = \frac{\int_0^{T_p} S_{\mathrm{Pr}o}(t) S^*_{\mathrm{Ref}}(t-\tau)dt}{\sqrt{\left(\int_0^{T_p} |S_{\mathrm{Pr}o}(t)|^2\right)\left(\int_0^{T_p} \left|S^*_{\mathrm{Ref}}(t)\right|^2\right)}} \tag{1}$$

In the above formula, $S_{\mathrm{Pr}o}(t)$ represents the ranging code of the actual satellite signal, the reference signal $S_{\mathrm{Ref}}(t)$ represents the ideal signal copy code generated by the local receiver, the symbol $*$ represents the conjugate operation, and the integration time T_p is a main code period of the reference signal. Use the correlation loss of the actually measured correlation curve, the receiver code loop phase detection curve deviation (S-curve Bias, SCB), and the S-curve slope deviation to evaluate the distortion of the correlation peak [1, 7].

a) Related Loss [2, 7].

The correlation loss is the difference between the actual received signal power of the signal and the ideal signal power. The expression for solving the correlation loss is:

$$\begin{aligned} P &= \max_{over\ all\ \varepsilon} (20\log_{10}(|CCF(\varepsilon)|)) \\ PCL[dB] &= P_{ideal} - P_{real} \end{aligned} \tag{2}$$

Where P is the signal power, P_{ideal} is the ideal signal power, P_{real} is the actual received signal power, and PCL is the relative loss.

b) S-curve Bias (SCB).

The zero-crossing point of the ideal S curve should be located at the position where the phase of the phase discrimination curve does not deviate. In fact, due to the influence of channel transmission distortion, the code loop phase discrimination curve is often locked at the position where the phase is deviated [4]. Taking the incoherent lead minus lag phase detector as an example, set the lead minus lag distance of the correlator as, then the S curve can be expressed as:

$$S(s_{out}, s_{in,k}, \varepsilon) = [CF(s_{out}, s_{in,k}, \varepsilon + \delta/2)^2 - CF(s_{out}, s_{in,k}, \varepsilon - \delta/2)^2] \tag{3}$$

In the above formula, CF represents the related function:

$$CF(\tau) = \int_0^{T_p} S(t)S^*(t-\tau)dt \tag{4}$$

Locking point deviation satisfies

$$SCurve(\varepsilon_{bias}(\delta), \delta) = 0 \tag{5}$$

The lock-in point deviation satisfies that when there is more than one zero-crossing point (such as BOC modulation signal), the zero-crossing point closest to the maximum relevant power should be selected. S-curve deviation is defined as:

$$SCB = \max_{overall\ \delta}(\varepsilon_{bias}(\delta)) - \min_{overall\ \delta}(\varepsilon_{bias}(\delta)) \tag{6}$$

The δ value range is $[0, \delta_{\max}]$, and the $\delta_{\max}$ values are as follows:

$$\delta_{\max}[chips] = \begin{cases} \dfrac{1.5}{4\frac{m}{n} - 1} BOC(m, n) \\ 1.5\, BPSK - n \end{cases} \tag{7}$$

From (6) and (7), the variation curve of the lock point deviation $\varepsilon_{bias}(\delta)$ with the distance δ can be obtained.

2.4 Modulation Characteristics

The modulation characteristics of the signal mainly analyze the effective power ratio deviation of the signal components and the carrier phase deviation between the signal components. The calculation process of the effective power ratio deviation of the signal components is as follows: First, the collected signal is filtered and demodulated to obtain the baseband signal. Then use Eq. (8) to calculate the correlation function between the local code generator and the received baseband signal, and calculate the power value of the signal. The power ratio of each signal component is:

$$E(j) = (\frac{1}{N}\sum_{i=1}^{N}\sqrt{(P_{Ii}^2 + P_{Qi}^2)})^2 \tag{8}$$

The statistical number of power ratios can be selected as the number of code cycles for a period of time, expressed as a percentage of the total power of a single signal. Calculate the carrier phase deviation between signal components based on the tracked data. Use the signal components after stable tracking to recover the complete carrier phase, compare the phase difference of each signal component with the relative phase value of the ideal signal component, and count the data for a period of time. The carrier phase deviation is the carrier between the signals. The maximum value of the absolute value of the relative phase error [7].

3 GNSS Signal Quality Index System

Satellite operation after launching requires continuous ground monitoring to ensure the quality and level of signal service. The ground monitoring system generally consists of an antenna unit, radio frequency channel unit, baseband processing unit, time-frequency reference unit, acquisition/playback storage unit, and integrated The control processing software unit is constituted together. As shown in Fig. 2.

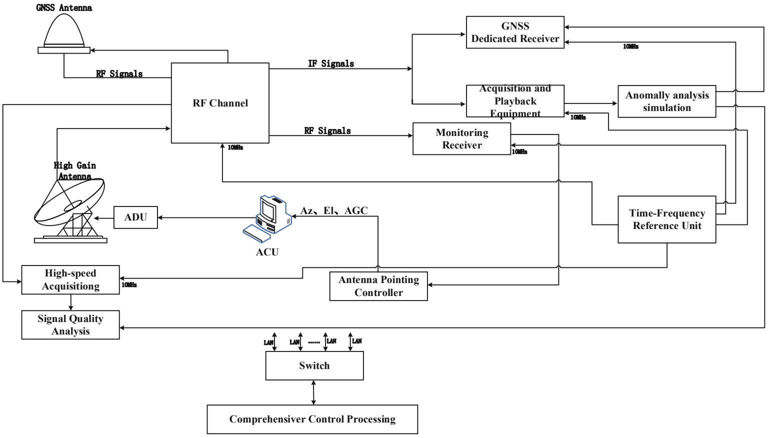

Fig. 2. GNSS satellite real-time on-orbit monitoring system block diagram.

The composition of signal quality analysis based on intelligent processing is shown in the Fig. 3 below.

GNSS satellite in-orbit intelligent signal quality monitoring composition block diagram. The omnidirectional antenna completes the reception of all GNSS signals, and the receiver realizes the reception and processing of the signals to analyze the continuous performance of the signal, ranging performance and other indicators, and judge the availability of the signal, The stability of the phase center of the antenna directly determines the accuracy level of the signal evaluation. This system uses the GNSS-750 four-system GNSS choke antenna in the design, and supports GPS, GLONASS, Galileo and Beidou. GNSS-750 has strong multi-system signal receiving ability and is suitable

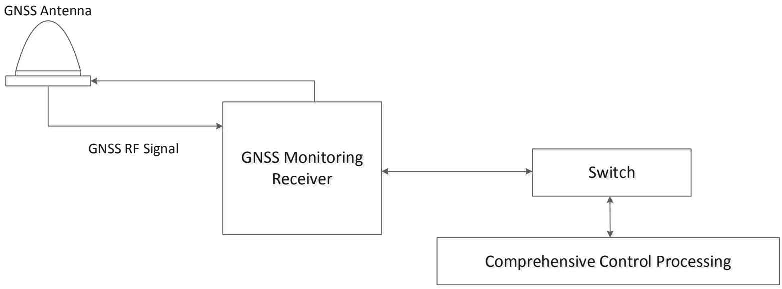

Fig. 3. Block diagram of GNSS satellite intelligent signal quality monitoring.

for application fields such as the construction of ground reference stations and geological monitoring.

High-gain antennas are used to monitor and process the signal quality of a single satellite. Since signal quality monitoring and analysis require relatively high signal carrier noise, high-gain antennas must be used to achieve this. The use of GNSS high-gain antennas can be very good Realize the evaluation of the signal quality, the monitoring receiver completes the calculation of the position information through the position information of a currently selected tracked satellite, and then converts the calculation of the pointing control system into the driving command of the ACU to complete the high-gain antenna The alignment and tracking action of the currently selected satellite.

3.1 Radio Frequency Channel Unit

The function of the radio frequency channel unit is to complete the processing of amplification, filtering, frequency conversion and power division of the signals output by the two antenna feed elements, so that the output signal frequency and power can be adapted to the input range of the back-end baseband processing unit. Figure 4 shows the principle block diagram of the radio frequency channel unit.

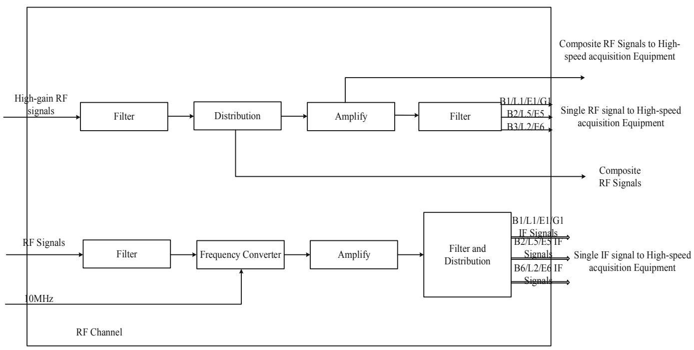

Fig. 4. Block diagram of the realization of the RF channel unit.

For the combined RF signal output by the high-gain antenna, the RF channel unit first filters it to suppress out-of-band interference. The filtered signal is then divided into two channels, and one channel is directly output to the GNSS monitoring receiver for receiving processing. One signal also needs to be amplified. The amplification gain is about 70 dB, and the amplified signal level range is about −30–0 dBm. The amplified signal is directly output as a combination and can be provided to high-speed acquisition equipment for direct sampling. The other amplified signal is then subjected to band-pass filtering, and three independent RF signals of B1/L1/E1, B2/E5/L5, B3/E6/L2 are filtered out from the combined signal, and the purpose is to purify the signal. To ensure the quality of signal acquisition, the branched radio frequency signal is still provided to the high-speed acquisition and storage device for subsequent processing. For the combined RF signal output by the omnidirectional antenna, it is also filtered to suppress out-of-band interference. The filtered signal needs to be down-converted. The converted signal is amplified (amplification gain is about 90 dB). The amplified 3 channels of IF signals are further processed by power division filtering. Each frequency signal is divided into 13 channels, of which 12 channels are provided to the BD dedicated receiver for baseband processing, and the other channel is output to the IF acquisition and playback storage device for completion. Continuous real-time collection of records.

3.2 GNSS Monitoring Receiver

As a high-precision measurement device, the monitoring receiver simultaneously observes the Beidou satellite signal in the field of view to obtain precise pseudorange, carrier phase, navigation message and other information, for the system satellite-ground time synchronization, precise orbit determination, and ionospheric propagation Delay correction and integrity monitoring provide observation data. Its key design indicators such as pseudorange measurement accuracy and carrier measurement accuracy are better than or equivalent to the current international advanced measurement receivers. In order to ensure stable operation in the increasingly complex electromagnetic environment in the future and ensure receiving performance, interference monitoring and suppression are A necessary function for monitoring receivers.

Through the GNSS receiver, the uninterrupted monitoring of the full system signals of 12 visible satellites can be completed in parallel in real time. On the basis of completing the monitoring of conventional observations, the expansion and improvement of monitoring items can be realized, especially the correct channel coding of the downlink signal. Performance verification and the analysis and processing functions of the original message, and at the same time, the automatic monitoring capability is improved from the software level, so that the efficiency of the entire monitoring system has been greatly improved.

The GNSS receiver includes 12 baseband signal processing boards, as well as a high-performance workstation. One of the baseband boards jointly completes the reception and processing of the full system signal of a single GNSS satellite, which can be regarded as a single-satellite receiver.

The basic block diagram of the baseband processing board is shown in Fig. 4. The baseband processing board includes a receive channel and a transmit channel. The receive channel includes 6 ADCs (ADS5402), and the transmit channel includes 4 DACs

(AD9736). It uses an external clock source and trigger signal., The receiving channel and the sending channel each correspond to a set of FPGA (XC5VLX330) and DSP (TMS32C6713B) devices, and both FPGA and DSP chip have expanded high-speed memory. A piece of TMS320C6455 processor implements CPCI bus and gigabit network interface, the EMIFA interface of TMS320C6455 is connected to two pieces of FPGA, and a piece of CPLD device is designed to control the hardware logic on the board. TMS320C6455 is designed with FLASH devices outside the chip for curing procedures. There are 10 pairs of bidirectional LVDS channels designed between the two FPGAs to facilitate data transmission between each other. Both FPGAs are designed with 10 pairs of bidirectional LVDS channels connected to the CPCI J3 and J5 connectors respectively for high-speed data between boards. transmission. Each FPGA is designed with one UART connected to the CPCI J3 connector, and each FPGA is designed with 32 single-ended signals connected to the CPCI J4 connector (Fig. 5).

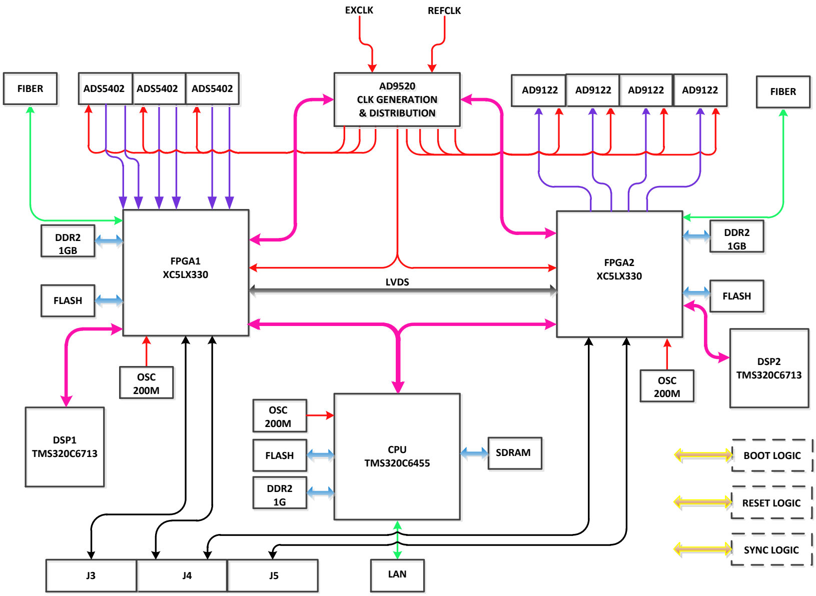

Fig. 5. Block diagram of the realization of the baseband signal processing boards.

The CPCI hardware board is shown in the figure. The two TMS320C6713Bs communicate through the McBSP interface. The EMIF and HPI interfaces of the two TMS320C6713Bs are connected to the corresponding FPGA. The HPI interface is mainly used to implement the host loading of the TMS320C6713B program. The programs of the two TMS32C6713B are solidified on the FLASH device on the board, and are automatically loaded when the board is powered on. The baseband processing board is integrated in a standard 4U-8 slot CPCI chassis for use, which facilitates the maintenance and upgrade of the equipment. A group of FPGAs and DSPs corresponding to the receiving channel on the board complete the baseband receiving and processing of the entire navigation signal, and a group of FPGAs and DSPs corresponding to the transmitting channel complete the generation of zero-value baseband signals. The C6455 on the board is responsible for completing the communication and control between the entire baseband board and the external network port.

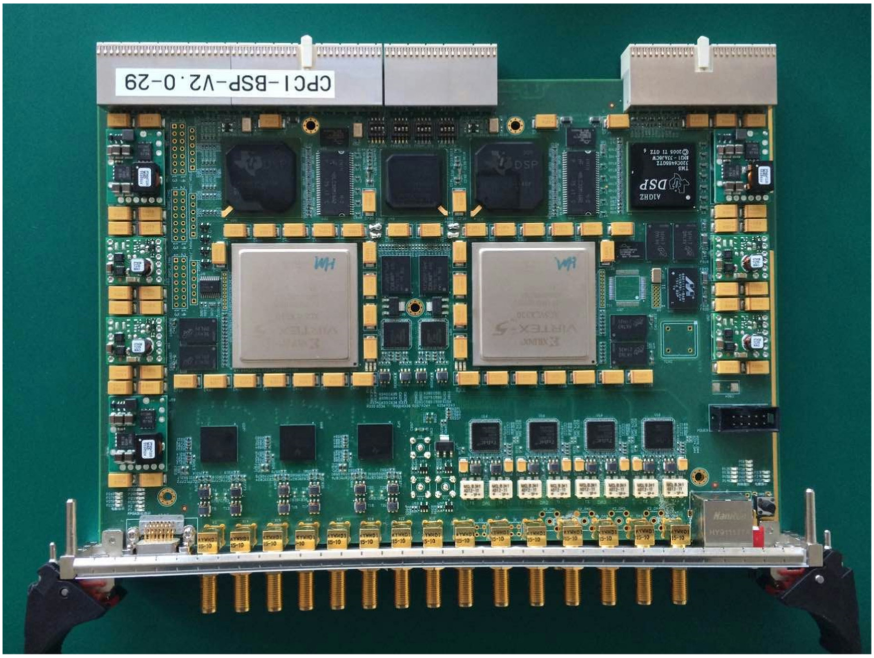

Fig. 6. Physical image of baseband signal processing board.

4 Intelligent Signal Quality Analysis Process Design

In addition to monitoring receivers for on-orbit monitoring of GNSS signals, the signal quality indicators described above require signal quality analysis software. The function of the signal quality analysis module is relatively independent, and the core is to realize the high-precision analysis and evaluation of data under the condition of high sampling rate through the idea of software receiver. Due to the huge amount of data and the complex processing algorithm, the quality analysis is realized by non-real-time post-processing, as a functional module of the comprehensive control software to realize the corresponding functions.

Figure 6 shows a block diagram of the software processing flow of the signal quality analysis module. First, the working mode is completed through the top layer, and the simulation analysis frequency point, sampling rate, simulation time and other working parameters are set. The signal quality analysis module will control the signal according to the given conditions. The way to read in. After the signal is captured, it enters the tracking loop. Through closed-loop analysis, the precise pseudo-code phase, carrier phase, data path integral value and other intermediate parameters of each signal component are obtained. Then, the system will use the code phase and carrier phase after stable tracking to correct the signal, and calculate its power spectrum, EVM index, constellation diagram, IQ orthogonality, and amplitude imbalance. Finally, all the intermediate parameters are processed, the pseudo-code mutual difference of each signal component, the phase deviation of the signal component and other indicators are calculated, and all the results are drawn and displayed.

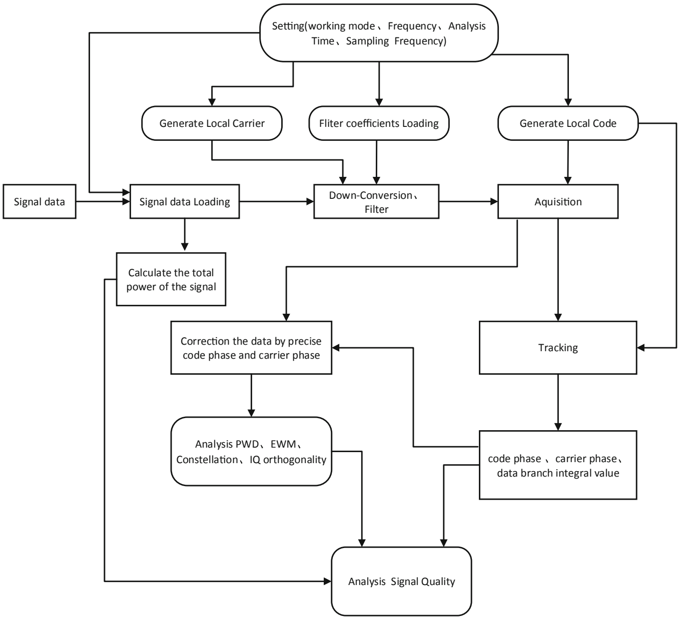

Fig. 7. Intelligent processing flow for signal quality analysis

Navigation signal quality parameters are divided into two categories. The first category is typical communication system parameters, including power spectral density, constellation diagrams, and eye diagrams; the second category is closely related to navigation, including code power, autocorrelation function shape, and correlation Loss, S-curve offset, multi-channel pseudo code consistency, pseudo code and data delay consistency, amplitude/phase frequency transfer characteristics, etc.

The signal quality parameter needs to process baseband signal samples up to tens of seconds to obtain the instantaneous transmission distortion characteristic of the navigation signal.

The power spectrum analysis usually uses the Welch periodogram method. The Welch periodogram method uses an improved average periodogram method to estimate the power spectrum of a random signal. It uses signal segment overlap, windowing, FFT and other techniques to calculate the power spectrum. The Welch method can improve the smoothness of the spectrum estimation curve and increase the resolution of the spectrum estimation. Comparing the measured power spectrum of the signal with the ideal power spectrum can check the power spectrum characteristics of the signal.

In the process of data analysis, use eye diagrams to observe the effects of inter-symbol crosstalk and noise. After filtering, demodulating, and Doppler frequency shift removal on the collected original data, the initial phase is used as the starting point, and the time-domain waveform diagram Repeatedly draw multiple chip data in.

The constellation diagram is used to analyze the characteristics of the signal modulation domain and calculate the signal quadrature modulation parameters. The constellation diagram is a diagram that represents the digital signal in the complex plane and visually shows the signal and the relationship between the signals. The constellation diagram needs to remove the Doppler effect. The reason why the digital signal can be represented by points on the complex plane is because the digital signal itself has a complex expression. Although the signal generally needs to be modulated to a higher frequency carrier for transmission, the final detection is still carried out on the baseband.

5 Test and Verification Results

This on-orbit monitoring system realizes the intelligent monitoring of GNSS satellite on-orbit signals, and improves the efficiency and real-time performance of monitoring processing. This system is deployed at the monitoring station, and has completed multiple GNSS signal monitoring and evaluation. Take the one-star evaluation result of the Compass system as an example. The evaluation results are shown in the following table. Through the evaluation, this system can realize the GNSS signal Flexible and intelligent monitoring, all indicators truly reflect the status of the satellite in orbit, and the statistics of the monitoring results are shown in the Table 1 below.

Table 1. Compass signals on-orbit monitoring and evaluation results.

Signal	Corrlation loss	S-curve bias	Time-domain bias
B1Cp	−0.102	0.111	0.803
B1Cd	−0.137	0.092	0.837
B1I	0.368	0.004	−0.115
B2ad	0.197	0.123	0.065
B2ap	0.190	0.125	0.002
B2b_I	0.161	0.051	−0.029
B2b_Q	0.176	0.051	−0.012
B3I	0.035	0.015	−0.115

In addition to the above relevant domain indicators, the system has qualitatively analyzed the time domain waveforms, constellation diagrams and eye diagrams. Figure 7 is the power spectral density, and Fig. 8 is the difference between the analyzed actual time domain waveform and the theoretical time domain waveform. Figure 9 shows the eye diagrams of various different signals. The entire analysis and processing process is automated (Fig. 10).

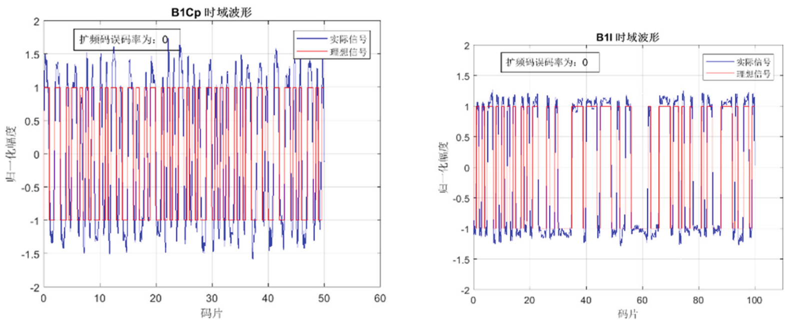

(a) B1 Signal (b) B2 Signal

Fig. 8. Power spectral density of GNSS signal

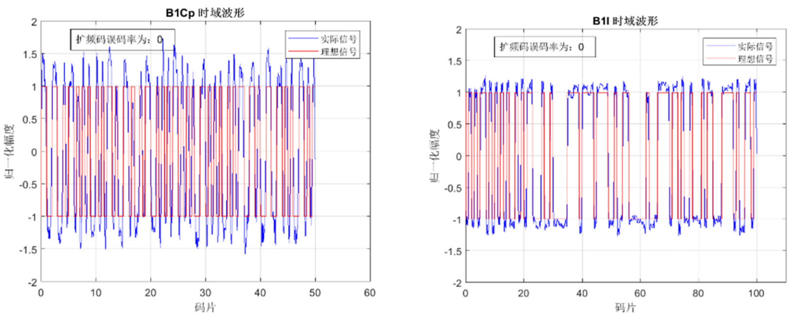

(a) B1Cp Signal (b) B1I Signal

Fig. 9. Time-domain waveform monitoring results of some signals

Judging from the test results, this system has well realized the on-orbit signal quality monitoring and analysis, and can meet the system requirements in terms of monitoring efficiency and monitoring performance.

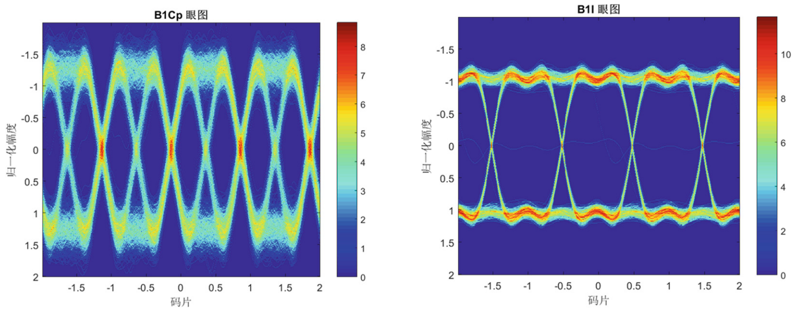

(a) B1Cp Signal (b) B1I Signal

Fig. 10. Partial signal eye diagram monitoring results

6 Conclusion

This paper introduces the design of an intelligent-based on-orbit monitoring system for GNSS signal quality. It gives a detailed introduction to the intelligent workflow, processing methods, system composition and other aspects of the system. Through on-orbit monitoring and analysis, this system can be very good. The improved monitoring efficiency provides a reference and reference for the monitoring of the performance of multiple GNSS systems, and has greater engineering application value.

References

1. Yang, Z., Xu, Q., Han, H.: Research on Pre-distortion Method of Navigation Satellite Launch Channel, CSNC (2016)
2. Soellner, M., Kohl, R., Luetke, W.: The impact of linear and non-linear signal distortions on Galileo code tracking accuracy. Pac. J. Math. **162**(1), 27–44 (2002)
3. Li, X., Ge, M., Lu, C., et al.: High-rate GPS seismology using real-time precise point positioning with ambiguity resolution. IEEE Trans. Geosci. Remote Sens. **52**(10), 6165–6180 (2014)
4. Soellner, M., Kurzhals, C., Hechenblaikner, G., et al.: GNSS offline signal quality assessment. In: Proceedings of International Technical Meeting of the Satellite Division of the Institute of Navigation, pp. 909–920 (2008)
5. Betz, J.W., Corporation T M: Effect of linear time-invariant distortions on RNSS code tracking accuracy. In: Proceedings of International Technical Meeting of the Satellite Division of the Institute of Navigation, pp. 1636–1647 (2002)
6. Falcone, M., Lugert, M., Malik, M., et al.: GIOVE-a in orbit testing results. In: Proceedings of International Technical Meeting of the Satellite Division of the Institute of Navigation (2006)
7. Felhauer, T.: On the impact of RF front-end group delay variations on GLONASS pseudorange accuracy. In: Proceedings of International Technical Meeting of the Satellite Division of the Institute of Navigation, pp. 1527–1532 (1997)